Talanta 130 (2014) 96–102

Contents lists available at ScienceDirect

Talanta

journal homepage: www.elsevier.com/locate/talanta

Sensitive electrochemical detection of NADH and ethanol at low potential based on pyrocatechol violet electrodeposited on single walled carbon nanotubes-modified pencil graphite electrode

Jun Zhu, Xiao-Yan Wu, Dan Shan*, Pei-Xin Yuan, Xue-Ji Zhang*

School of Environmental and Biological Engineering, Nanjing University of Science and Technology, Nanjing 210094, China

ARTICLE INFO

Article history:
Received 2 February 2014
Received in revised form
21 June 2014
Accepted 25 June 2014
Available online 3 July 2014

Keywords:
Pyrocatechol violet
Single-walled carbon nanotubes
Pencil graphite electrode
Dihydronicotinamide adenine dinucleotide
Ethanol

ABSTRACT

In this work, the electrodeposition of pyrocatechol violet (PCV) was initially investigated by the electrochemical surface plasmon resonance (ESPR) technique. Subsequently, PCV was used as redox-mediator and was electrodeposited on the surface of pencil graphite electrode (PGE) modified with single-wall carbon nanotubes (SWCNTs). Owing to the remarkable synergistic effect of SWCNTs and PCV, PGE/SWCNTs/PCV exhibited excellent electrocatalytic activity towards dihydronicotinamide adenine dinucleotide (NADH) oxidation at low potential (0.2 V vs. SCE) with fast amperometric response (< 10 s), broad linear range (1.3–280 μM), good sensitivity (146.2 μA mM^{-1} cm^{-2}) and low detection limit (1.3 μM) at signal-to-noise ratio of 3. Thus, this PGE/SWCNTs/PCV could be further used to fabricate a sensitive and economic ethanol biosensor using alcohol dehydrogenase (ADH) via a glutaraldehyde/BSA cross-linking procedure.

1. Introduction

Dihydronicotinamide adenine dinucleotide (NADH) and its oxidized form nicotinamide adenine dinucleotide (NAD^+) are significant coenzymes which participates in a variety of enzymatic reactions via more than 300 dehydrogenases [1]. Therefore many studies have focused on the electrochemical oxidation of NADH to develop NAD^+-dependent enzymatic biosensors using for environmental, food control, clinical analysis [2,3]. However, the direct oxidation of NADH at conventional electrodes requires a high overpotential positive of 0.6–0.8 V vs. SCE [4] and suffers from low sensitivity and the fouling of the electrode surface by its oxidation products, which cause loss of selectivity, reproducibility and stability [5,6].

Considerable effort has been devoted to identify new electrode materials or efficient electron-transfer mediators as the catalysts to allow the electrochemical determination of NADH at low potential, e.g. azine dyes [7,8], quinones [9], metal nanoparticles [10,11] and carbon nanomaterials [12,13]. Carbon nanotubes (CNTs) have received considerable attention for this purpose. Many studies have demonstrated that CNTs can be used to fabricate the nanostructured macroscopic electrodes, biosensors, and nanobioelectronic devices due to their nanometer size, lack of toxicity, good electrocatalytic properties, and efficient accumulation of biomolecules as well as minimization of surface fouling [14]. Furthermore, endowment SWCNTs with redox properties could efficiently accelerate the oxidation speed of NADH [15].

The purpose of this work is to develop the electrocatalysis of NADH and to fabricate an enhanced performance ethanol biosensor. Pyrocatechol violet (PCV) is used as mediator and electrodeposited on the SWCNTs-modified pencil graphite electrodes (PGEs). PCV is a sulfone phthalein dye prepared from condensing two moles of pyrocatechol with one mole of *o*-sulphobenzoic acid anhydride. It has been demonstrated that materials from catechol and gallate families, containing OH groups bonded to the adjacent carbon atoms of the aromatic ring, strongly adsorbed on various inorganic materials. It is important to note that such bonds improved charge transfer between inorganic and organic materials [16]. Moreover, SWCNTs exhibit a special sidewall curvature and possess a π-conjugative structure, which allows them to interact with PCV through π–π electronic interactions.

PGE was applied due to the following advantages: (a) high electrochemical reactivity with a wide polarized potential domain in aqueous solutions; (b) a variety of easy methods of surface modification by electrochemical, chemical and mechanical treatment; (c) high stability at slightly degraded surface activity;

* Corresponding authors. Fax: +86 25 84303107.
E-mail addresses: danshan@njust.edu.cn (D. Shan), xueji@usf.edu (X.-J. Zhang).

http://dx.doi.org/10.1016/j.talanta.2014.06.057
0039-9140/

(d) low cost and usable as disposable electrochemical tool; and (e) a renewal surface which is simpler and faster than polishing procedures, common with solid electrodes, and results in good reproducibility for the individual surfaces [17,18]. Thus, recently many scientists have focused on the use of these electrodes in various electroanalytical applications due to the useful properties of PGEs [19–21].

In addition, PCV electrochemical deposition was investigated initially by electrochemical surface plasmon resonance (ESPR).

2. Experimental

2.1. Reagents

Alcohol dehydrogenase (ADH) (EC 1.1.1.1, from *Saccharomyces cerecisiae*, ≥ 300 units mg^{-1}), β-nicotinamide adenine dinucleotide reduced disodium salt hydrate (NADH), β-nicotinamide adenine dinucleotide sodium salt from *S. cerevisiae* (NAD^+) and bovine serum albumin (BSA) were purchased from Sigma. Procatechol violet (PCV) was obtained from Sangon Chemicals (China). Single-wall carbon nanotubes (SWCNTs), produced by HiPco® process (Purified, CNI grade, lot no. Po313), were purchased from Carbon Nanotechnologies, Inc. and were further functionalized as described earlier [22]. The chemically modified SWCNTs were dispersed in distilled water leading to a concentration of 0.1 mg ml^{-1}. All other chemicals were of analytical grade and used without further purification. Phosphate buffer solution (PBS) was 0.1 M K_2HPO_4 and KH_2PO_4 and its pH was adjusted with H_3PO_4 or KOH solutions. Twice-distilled water was used throughout the experiment. Beers and liquors were purchased in local supermarkets.

2.2. Apparatus and instrumentations

A CHI 660D electrochemical workstation (CH Instrument) was used for cyclic voltammetry and amperometric measurements. All electrochemical studies were performed with a conventional three electrode system. A saturated calomel electrode (SCE) and a Pt wire electrode were used as reference and counter electrodes, respectively. All the potentials mentioned below are relative to SCE. The working electrode was a home-made pencil graphite electrode (PGE). The pencil leads were obtained from Dena Co. Ltd., China. All leads had a total length of 85 mm and a diameter of 2 mm. The pencil leads were used as received. The morphology of the modified electrodes was investigated with a XL-30E scanning electron microscope (SEM). Static water contact angle measurements were performed by the sessile drop technique using an Optical Tensionmeter (Theta Lite, Finland), under ambient laboratory conditions. A drop of distilled water was applied to the surface of bare and modified PGE, and the contact angle measurements were carried out within 30 s of the contact. An ESPRIT instrument (Echo Chemie B.V., Ultrech, Netherlands) was used to perform the optical measurements of the Surface Plasmon Resonance (SPR) angle and cyclic voltammetry was carried out with a potentiostat (AUTOLAB) from Echo Chemie (Utrecht, Netherlands). The ESPRIT instrument is based on the Kretschmann configuration [23] with a scanning-angle setup. In this system, the intensity of reflected light is minimum in the resonance angle. This angle can be measured over a range of 4° in this equipment by using a photodiode detector. The incidence angle was varied by using a vibrating mirror (rotating over an angle of 5° at 77 Hz in 13 ms), which directs p-polarized laser light onto a 1 mm $\times$ 2 mm spot of the sensor disk via the hemicylindrical prism of BK7 glass. In each cycle, the reflective curves were scanned on both forward and backward movements of the mirror. In this vibrating mirror set-up, the resolution was 1 m°. The light source (LASER) of the system is composed of the laser diode with emission wavelength of 670 nm. In the experiments, a gold sensor disk containing a hemicylinder was mounted into a precleaned SPR cuvette. In order to obtain high inertness, it was made of Teflon®. The solutions were injected into the cuvette using a syringe with a stainless steel needle (Fig. 1). In order to avoid contamination on gold surface between the polymerization experiments was adopted the procedure previously reported [24]. The SPR angle shifts ($\Delta\theta$) were converted into mass uptake using a sensitivity factor of 120 mdeg (milli-degrees) corresponding to 100 ng cm^{-2} of molecular loading, and the MW of each immobilized molecule [25].

The determination of ethanol contents in wine samples was performed on an Agilent 6890N GC equipped with a FID (Palo Alto, CA, USA). An Agilent HP-INNOWAX capillary column (30 m $\times$ 0.32 mm i.d., film thickness 0.1 μM) was employed for separation. Ultra-high purity (99.999%) nitrogen was used as the carrier gas at flow rate of 1.0 mL/min. The injection volume was 1.0 μL and all the injections were performed in a split ratio of 1:10. The column temperature was set isothermally at 90 °C. The injector and detector temperatures were at 250 and 280 °C, respectively.

2.3. Preparation of SWCNTs, PCV and SWCNTs/PCV modified electrodes

A pencil graphite electrode (PGE) was polished carefully with 0.05 μm alumina particles on silk followed by sonication in deionized water and ethanol, and dried in air prior to use. The modification of PGE with SWCNTs was performed by casting 4 μl of SWCNTs aqueous solution (0.1 mg ml^{-1}) on the electrode surface and dried in air. The electrochemical deposition of PCV as performed over the surface of bare PGE and PGE/SWCNTs, respectively, in a 0.1 M PBS (pH 7) containing 1 mM PCV and 0.1 M KCl, through cyclic voltammetry between -0.2 and 0.5 V for 20 cycles at a scan rate of 20 mV s^{-1}. The modified electrodes obtained above were denoted as PGE/PCV and PGE/SWCNTs/PCV, respectively.

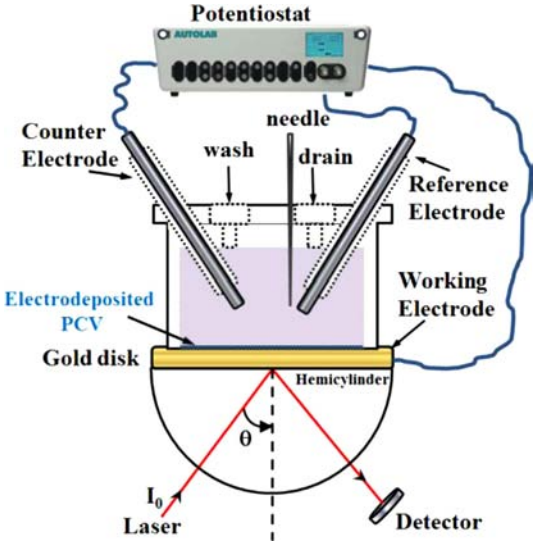

Fig. 1. Schematic diagram of SPR spectroscopy using the Kretschmann configuration. The light source (laser) of the SPR system is composed of a laser diode with an emission wavelength of 670 nm. A scanning mirror with a frequency of 76 Hz was used to obtain an angle scan of 4000 m° in approximately 13 ms. θ represents the angle of incident light.

2.4. Preparation of ethanol biosensor

ADH was immobilized on the PGE/SWCNTs/PCV by a glutaraldehyde/BSA cross-linking procedure. The ADH (3 mg) was dissolved in 100 μL of 0.1 M PBS (pH 7.5) containing 4 mg BSA. Then the glutaraldehyde (2.5% w/v), which is a bifunctional cross-linking agent, was added to the ADH solution up to a final concentration of a 0.9% w/v. In the process, the mixture was stirred thoroughly. The PGE/SWCNTs/PCV was dipped into this solution for 3 s and then removed. The enzyme electrode was placed in a desiccator for some time to allow the gel formation. This procedure was repeated four times. The resulting enzyme electrode (defined as PGE/SWCNTs/PCV/ADH) was stored in 0.1 M PBS (pH 7.5) at 4 °C for 4 h before use.

3. Results and discussion

3.1. ESPR measurement for the PCV electrodeposition

The electrodeposition was carried out by potential cycling between 0 and 0.9 V vs. SCE at 20 mV s^{-1} and the electrolytic solution consisting of 1 mM PCV and 0.1 M KCl in 0.1 M PBS (pH 3). As can be observed, the SPR angle position shifted toward more positive values during the voltammetric experiments (Fig. 2). The cyclic voltammograms (CVs) obtained during electrodeposition of PCV are shown in Fig. 2A up to 10th cycle. The double layer region of gold in 0.1 M PBS (pH 3) can be identified between the potentials of 0.0 V and 0.26 V. An anodic peak locates at 0.40 V in the first potential sweep, due to oxidation of catechol to *o*-benzoquinone [24]. A minor peak is observed around 0.69 V, which associated with the electrosorption of hydroxyl and /or oxygen species on gold and possibly also some PCV adsorption [26]. The dramatically large oxidation peak occurs at ~0.9 V corresponds formally to participation of two subsequent processes, the continuation of the gold surface oxidation and the PCV electrooxidation. The oxide formation occurs in the potential range from ca. 0.5 to 1.2 V with the growth of a quasi-three-dimensional structure of AuO [27]. The subsequent phenol oxidation is a complex process that takes place on the freshly formed gold oxide (AuO) and it may act as an intermediate in the organic oxidation and is called a surface-mediator. The first step of the phenol oxidation involves the formation of an adsorbed layer of phenoxy radicals on the surface-mediator [28]. Such radicals remain on the electrode surface and experience further oxidation forming possible many different products such as quinones, aliphatic acids, carbon dioxide [29], dimers and a surface polymeric film through coupling reactions involving adjacent phenoxy and dimeric radicals [30]. Further oxidation of PCV becomes more and more difficult because the diffusion of PCV molecules from the bulk solution towards the electrode surface has to take place through the layer of adsorbed catechols. This results in a shift of both oxidation and reduction peak potentials leading to overall increase in peak separation of the redox couple.

Fig. 2B presents the SPR response evolution in time during 10 potential scans in 0.1 M PBS (pH 3) containing 1 mM PCV and 0.1 M KCl. The amplitude of oscillation increases and achieves the steady value of about 218 ± 10 m° after 4 cycles. Subsequently, the SPR signal increases progressively with a slope of 1.07 m°/s or an average of accumulation rate of 90 ± 9 m°/cycle.

Fig. 2C presents the evolution of angular SPR reflectivity curve measured at 0.9 V, after each CV scan during characterization in 0.1 M PBS (pH 3) containing 1 mM PCV and 0.1 M KCl. The angle of resonance minimum of SPR curves shows also a large shift in the angle of resonance minimum of about 660 m° suggests that the potential induced changes on the surface and the increase in thickness for the film of the electrodeposited PCV. Nevertheless, the slight shape changes of the reflectivity curves may be related to the modified redox properties of electrode due to the PCV electrodeposition.

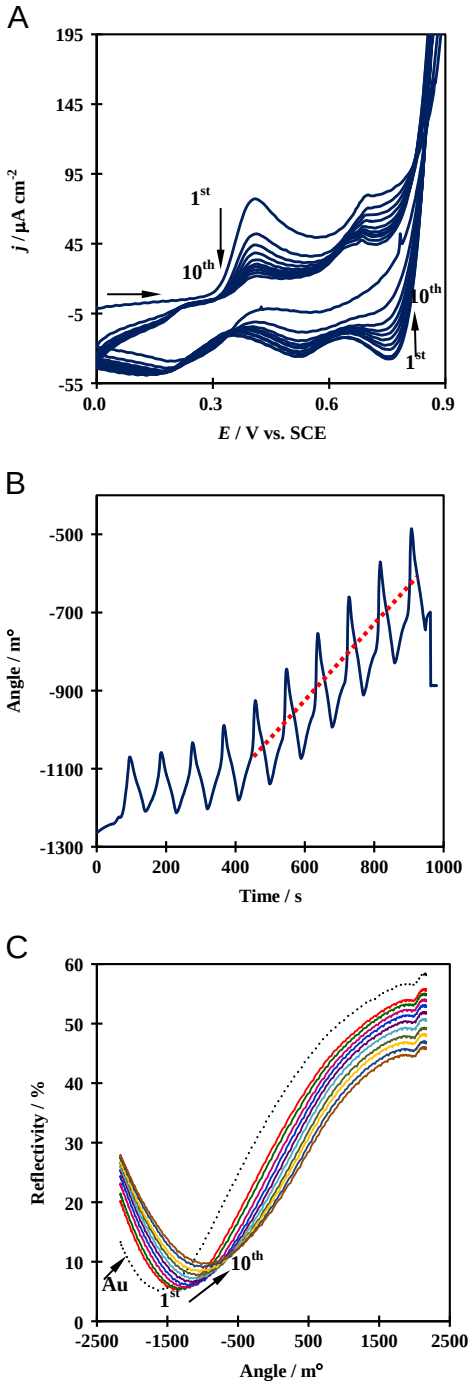

Fig. 2. (A) Cyclic voltammograms for PCV electrodeposition on Au-coated SPR sensor surface during electrolysis of PBS (0.1 M, pH 3) containing 1 mM PCV and 0.1 M KCl at scan rate of 20 mV s^{-1}. (B) The corresponding SPR response evolution in time during 10 potential scans for PCV electrodeposition. (C) The corresponding reflectivity vs. angle plots before (dashed line) and during 10 cycles for PCV electrodeposition recorded at 0.9 V. The SPR angle data have 5% of uncertainty.

3.2. Surface characterization

SEM technique was used to obtain direct visualization of bare PGE, PGE/PCV, PGE/SWCNTs and PGE/SWCNTs/PCV. The morphology of

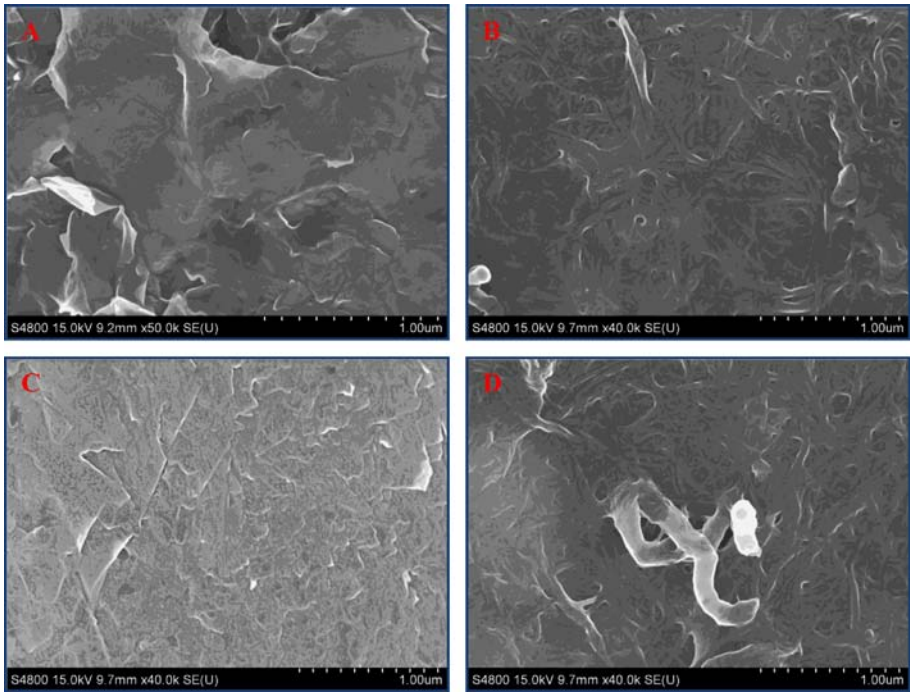

Fig. 3. SEM photographs of (A) PGE, (B) PGE/SWCNTs, (C) PGE/PCV and (D) PGE/SWCNTs/PCV.

bare PGE exhibits soft and rough surface with many curly damaged sheets of graphite (Fig. 3A). The surface of PGE/SWCNTs depicts the characteristic of SWCNTs with the entangled tubular structure (Fig. 3B). PCV electrodeposited on PGE results in a relatively compact surface coated with many globular microstructure (Fig. 3C). As for the case of PCV electrodeposited on PGE/SWCNTs, SWCNTs with enhanced diameter were well dispersed and incorporated with PCV films and an interconnected SWCNTs network formed on the electrode. This conductive SWCNTs network may establish electrical conduction pathways throughout the whole system, which is responsible for the electric conductivity and electrochemical sensing (Fig. 3D).

Static contact angle measurement directly on the surface of chemically modified electrodes can yield valuable information on solid/liquid interface especially in case of immobilized electroactive species as described by Murray et al. [31]. The contact angles were measured to be 72°, 66°, 78.5° and 60° for bare PGE, PGE/PCV, PGE/SWCNTs and PGE/SWCNTs/PCV, respectively. The decrease in the contact angle for PGE/SWCNTs/PCV may be ascribed to the cooperation of phenolic hydroxyl, sulfonic groups of deposited PCV and –COOH groups on the acid-pretreated SWCNTs. This enhanced hydrophilicity of interface for PGE/SWCNTs/PCV is expected to promote the electrochemical process taking place at the modified electrode surface.

3.3. Electrochemical response of modified electrode to NADH

The detection of NADH is of great important because it is produced in reactions that are catalyzed by hundreds of dehydrogenases. In order to test the potential electrocatalytic activities of the SWCNTs/PCV nanohybrids, cyclic voltammetric responses were recorded at those bare and modified electrodes in the absence and presence of NADH. With bare PGE, the oxidation of NADHs results in a broad wave and the maximum oxidation current can be found at 0.5 V (Fig. 4A). SWCNTs can dramatically lower the overpotential of NADH oxidation at the surface of electrode and facilitate electrochemical oxidation of NADH (Fig. 4B). As for the case of PGE/PCV, the onset potential of NADH oxidation is obtained at 0.03 V and a small peak emerges at 0.21 V (Fig. 4C). The further enhanced oxidation of NADH can be achieved feasibly by PGE/SWCNTs/PCV as shown in Fig.4D. The substantial negative shift with an onset potential is at −0.13 V and a low oxidation peak with larger current signal is at 0.15 V.

The amperometric measurement of the PGE/SWCNTs/PCV to NADH at an applied potential of 0.2 V upon successive addition of NADH into stirring 0.1 M PBS (pH 7.0) was performed. Upon the addition of an aliquot of NADH to the buffer solution, the oxidation current increases steeply to reach a stable value. The proposed modified electrode achieves 95% of the steady-state current within 10 s. The response to NADH is linear in the range from 1.3×10^{-6} to 2.8×10^{-4} M, and with a linear regression equation for j (μA cm^{-2})=146.2 [NADH] (mM)+1.445, R^2=0.993 (n=17). This analytical performance was compared to those recently reported in the literature for the NADH electrochemical detection (Table 1). It appears that at relatively low potential, the comparatively high sensitivity, low detection limit can be obtained with this economic PGE/SWCNTs/PCV. This developed analytical performance may be ascribed to the synergic effect of PCV electrodeposited on SWCNTs with good electron transfer, the improved wetting properties.

3.4. Electroanalytical aspects of oxidation of ethanol

The excellent sensitivity and high precision of the proposed sensor towards the detection of NADH make it attractive for the further development of dehydrogenase-based electrochemical sensors. The dehydrogenase enzymes catalyze the oxidation of a variety of substrates in the presence of cofactor NAD^+, which can be applied in sensors and biotransformation design [38]. Therefore, ADH was modified on the PGE/SWCNTs/PCV and the electrocatalytic activity of the ethanol biosensor was examined using cyclic voltammetry ranging from −0.2 to 0.5 V with the scan rate of 2 mV s^{-} in 0.1 M PBS (pH 7.5) containing 5 mM NAD^+. In the presence of 1 mM ethanol, a distinguished catalytic effect is observed: an enhancement of the oxidation current and a concomitant decrease of the cathodic current (inset A of Fig. 5).

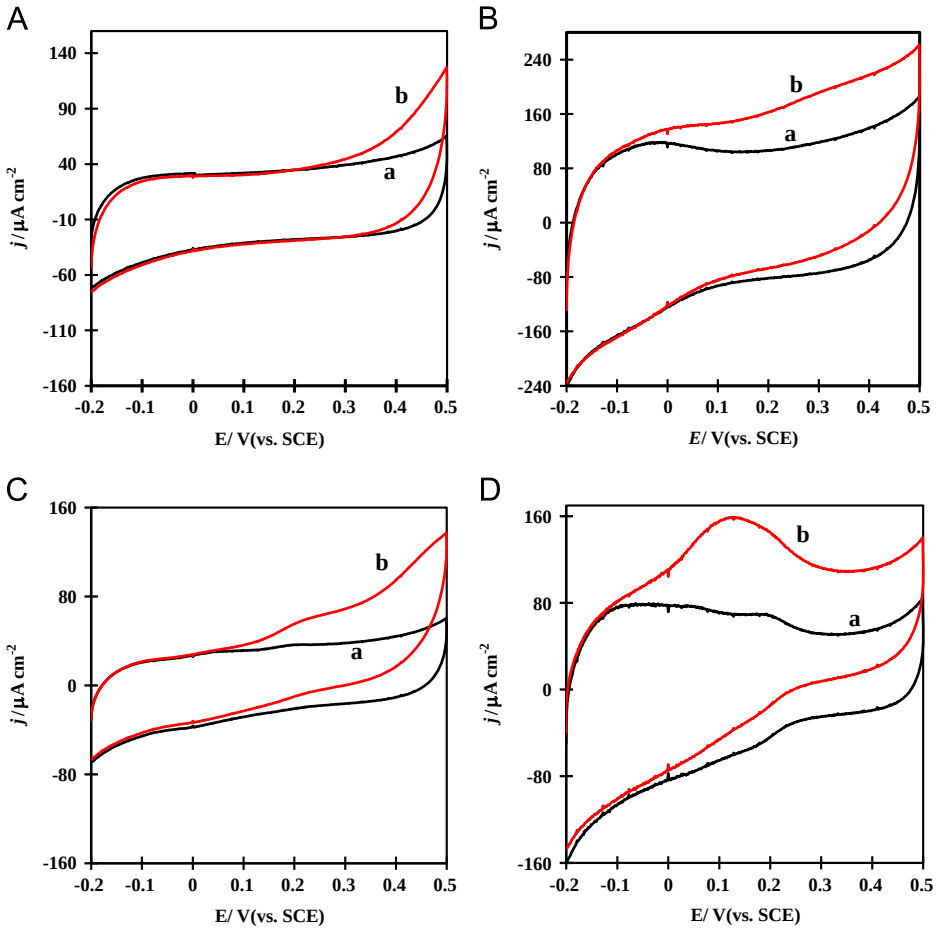

Fig. 4. Cyclic voltammograms of (A) bare PGE, (B) PGE/SWCNTs, (C) PGE/PCV and (D) PGE/SWCNTs/PCV in N_2-saturated PBS (0.1 M, pH 7) in the absence (a) and presence of 1 mM NADH (b), scan rate 2 mV s^{-1}.

Table 1
Analytical performance of other modified electrodes for NADH detection.

Electrode	E_{app} (V)	Sensitivity (μA mM^{-1} cm^{-2})	LR (μM)	LOD (μM)
PGE/SWCNTs/PCV	**0.2**	**146.2**	**1.3–280**	**1.3**
GCE/GO[a]/PDA[b]/AuNPs [32]	0.1	40.3	0.05–42	–
PD[c]/CNT/GC [15]	0	125.3	~50	1.8
IL-graphene[d]/chitosan/GCE [33]	0.45	37.4	250–2000	–
ERGO-PTH[e]/GC [34]	0.4	143	10–3900	10
PDAMS[f]/PtNPs/Pt [35]	0.3	68.2	~2500	4.8
PMDUS[g]/PtNPs/Pt [20]	0.3	40.2	~2100	6.2
GN-AuNRs[h]/GC [36]	0.4	10.3 27.1	20–160 160–480	6.0
MDB/GMCs/CS/SPE (pH 8) [37]	−0.15	148	10–410	0.19

[a] Graphene oxide.
[b] Polydopamine.
[c] 1,10-phenanthroline-5,6-dione.
[d] Ionic liquid-functionalized grapheme.
[e] Electroreduced graphene oxide (ERGO) and polythionice (PTH).
[f] Polydiallylmethylsilane.
[g] Polymethyldiundecenylsilane.
[h] Graphen–Au nanorods hybrid nanosheets.

Fig. 5 displays the amperometric response for successive addition of ethanol into a stirred 0.1 M PBS (pH 7.5) containing 5 mM NAD^+ recorded at the proposed biosensor under the operation potential of 0.2 V. Apparently, each addition of ethanol gives rise to a rise in current. The corresponding calibration curve is shown in inset B of Fig. 5. The anodic current increased linearly with ethanol concentration over the range from 9.3×10^{-6} to 3.2×10^{-4} M with a good sensitivity of 1.94 μA mM cm^{-2}. Five different ethanol biosensors were tested independently for the amperometric response to ethanol, providing a RSD value of 7.8%. The stability of the proposed ethanol sensor stored at 4 °C was investigated by recording periodically its current response to 1×10^{-4} M ethanol. The response of the biosensor was unchanged during the initial three weeks. It still retained about 76% of its original response after 52 days of storage. The effect of possible interfering species such as methanol, isopropanol, ascorbic acid and uric acid on ethanol detection has been examined (inset of Fig. 5C). No appreciable signals were observed for the successive injection of the interferents into the electrolyte solution.

To illustrate feasibility of the fabricated ethanol biosensor in practical analysis, the proposed ethanol sensor was used to detect ethanol concentration in three different alcoholic beverages: alcoholic beer, low alcohol content liquor and high alcohol content liquor. These alcoholic beverages were bought from the local supermarket. The pretreatment of these samples only requires a dilution step. Each sample was diluted with a phosphate buffer (0.1 M, pH 7.5) to a concentration within the working range of the biosensor. Table 2 depicts the analytical results of various commercial alcohol beverages. The accuracy of our biosensor method was also evaluated by comparison with the gas chromatographic method [39]. The relative errors are acceptable. The calculated results show that the results determined by biosensor were in satisfactory agreement with those given by the gas chromatographic method, indicating that it is feasible to apply the proposed biosensor to determine ethanol in real samples.

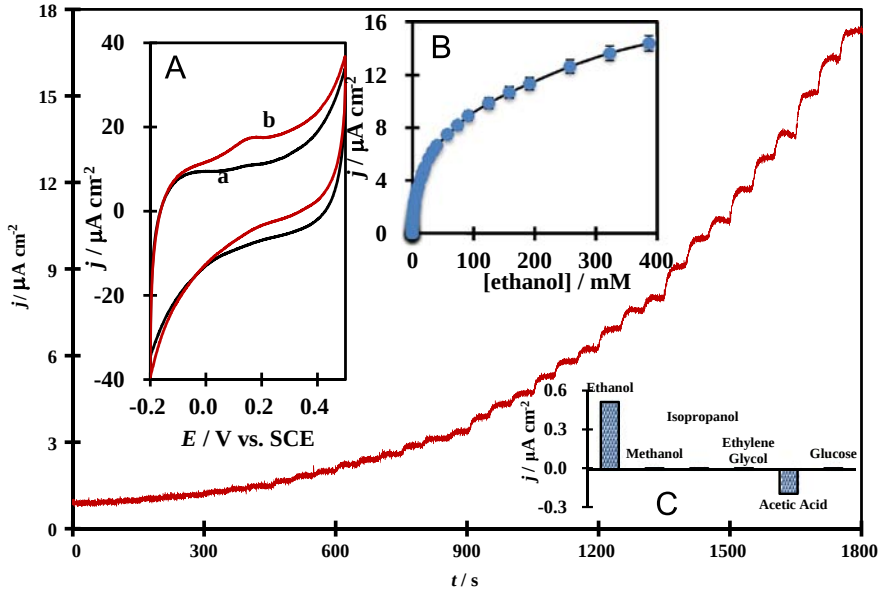

Fig. 5. Typical steady-state response of the ethanol biosensor on successive injection of ethanol into 5 ml of stirring 0.1 M N_2-saturated PBS (pH 7.5) containing 5 mM NAD^+, applied potential: 0.2 V vs. SCE. Inset A: Cyclic voltammograms of as-prepared ethanol sensor in 0.1 M PBS (pH 7.5) containing 5 mM NAD^+ in the absence (a) and presence of 1 mM ethanol (b), scan rate 2 mV s^{-1}. Inset B: The obtained calibration curves of the proposed ethanol sensor to ethanol. Inset C: The sensing selectivity of the proposed ethanol sensor to 2 mM ethanol, 2 mM methanol, 2 mM isopropanol, 2 mM ethylene glycol, 2 mM acetic acid, 0.2 mM glucose in a stirring 0.1 M PBS (pH 7.5) containing 5 mM NAD^+ with the applied potential of 0.2 V vs. SCE.

Table 2
Determination of ethanol in real samples with the proposed biosensor and comparison with gas chromatographic (GC) methods.

Sample	GC method (v/v)[a]	Biosensor (v/v)	RSD (%)
Alcoholic beer	3.25	3.34	2.69
Low alcohol content liquor	36.7	38.1	3.67
High alcohol content liquor	52.2	54.6	4.39

[a] Average of three measurements.

4. Conclusion

In summary, this work demonstrated that redox mediator PCV electrodeposited on SWCNTs modified PGE improved efficiently the ability for promoting electron transfer between the redox mediator and the electrode surface. Highly conductive SWCNTs can provide higher electrochemically accessible surface area for electrodeposition of a redox-active film of PCV with enhanced surface coverage. PCV electrodeposited on the SWCNTs-modified electrode can provide even higher porous 3D structure with enhanced hydrophilicity, which benefits the diffusion of the substrate. In addition, PGE/SWCNTs/PCV provides the attractive possibility to lowering the potential of NADH oxidation making them extremely promising candidates to serve as the electrochemical support for the incorporation of dehydrogenase enzymes. As a result, the strategy reported in this work for biosensing application can be expected to offer new prospects for the development of cheap, sensitive and selective sensors for clinical, pharmaceutical, environmental and forensics applications.

Acknowledgments

This work was supported by the National Natural Science Foundation of China (Grant no. 21175114), the Natural Science Foundation of Jiangsu (BK2011441 and BK20130754), Qing Lan project of Jiangsu province and NJUST Research Funding (Nos. 2011ZDJH17 and 2012ZDJH009), and the Fundamental Research Funds for the Central Universities (Nos. 30920130112012 and 30920140112009), PhD Fund of Chinese Ministry of Education for Young Teachers (0133219120019), and State Key Laboratory of Analytical Chemistry for Life Science (SKLACLS1302).

References

[1] H.C. Chang, X.J. Wu, C.Y. Wu, Y. Chen, H. Jiang, X.M. Wang, Analyst 136 (2011) 2735–2740.
[2] B. Limoges, D. Marchal, F. Mavré, J. Savéant, J. Am. Chem. Soc. 128 (2006) 2084–2092.
[3] T. Huang, A. Warsinke, T. Kuwana, F.W. Scheller, Anal. Chem. 70 (1998) 991–997.
[4] L. Li, H.M. Lu, L. Deng, Talanta 113 (2013) 1–6.
[5] M. Pumera, R. Scipioni, H. Iwai, T. Ohno, Y. Miyahara, M. Boero, Chem. A Eur. J. 15 (2009) 10851–10856.
[6] B.A. Deore, M.S. Freund, Chem. Mater. 17 (2005) 2918–2923.
[7] S.M. Wang, H.H. cheng, K.F. Kai, S.H. Cheng, Electrochim. Acta 77 (2012) 330–338.
[8] Y.C. Tsai, S.Y. Chen, H.W. Liaw, Sens. Actuators B: Chem. 125 (2007) 474–481.
[9] S. Liu, G. Dai, L. Yuan, Y. Zhao, J. Chin. Chem. Soc. 59 (2012) 1409–1414.
[10] C.H. Chen, Y.C. Chen, M.S. Lin, Biosens. Bioelectron. 42 (2013) 379–384.
[11] J.H. Shim, Y. Lee, M. Kang, J. Lee, J.M. Baik, Y. Lee, C. Lee, M.H. Kim, Anal. Chem. 84 (2012) 3827–3832.
[12] T.Y. Huang, J.H. Huang, H.Y. Wei, K.C. Ho, C.W. Chu, Biosens. Bioelectron. 43 (2013) 173–179.
[13] K. Guo, K. Qian, S. Zhang, J. Kong, C. Yu, B. Liu, Talanta 85 (2011) 1174–1179.
[14] H. Teymourian, A. Salimi, R. Hallaj, Talanta 90 (2012) 91–98.
[15] X.Y. Mao, Y.H. Wu, L.L. Xu, X.J. Cao, X.J. Cui, L.D. Zhu, Analyst 136 (2011) 293–298.
[16] X. Li, I. Zhitomirsky, J. Power Sources 221 (2013) 49–56.
[17] Z.O. Uygun, Y. Dilgin, Sens. Actuators B: Chem. 188 (2013) 78–84.
[18] Y. Dilgin, B. Kızılkaya, D.G. Kilgin, H.I. Gökçel, L. Gorton, Colloids Surf. B: Biointerfaces 102 (2013) 816–821.
[19] A.A. Ensafi, M. Amini, B. Rezaei, Biosens. Bioelectron. 53 (2014) 43–50.
[20] S.H. Wu, B.J. Zhu, Z.X. Huang, J.J. Sun, Electrochem. Commun. 28 (2013) 47–50.
[21] A. Erdem, G. Duruksu, G. Congur, E. Karaoz, Analyst 138 (2013) 5424–5430.
[22] M. Chen, J.Q. Xu, S.N. Ding, D. Shan, H.G. Xue, S. Cosnier, M. Holzinger, Sens. Actuators B: Chem. 152 (2011) 14–20.
[23] Á. Fekete, Int. J. Circuit Theory Appl. 41 (2013) 646–652.
[24] J. Zhu, D.S. Chauhan, D. Shan, X.Y. Wu, G.Y. Zhang, X.J. Zhang, Microchim. Acta 181 (2014) 813–820.
[25] N. Yang, X. Su, V. Tjong, W. Knoll, Biosens. Bioelectron. 22 (2007) 2700–2706.
[26] M. Ferreira, H. Varela, R.M. Torresi, G. Tremiliosi-Filho, Electrochim. Acta 52 (2006) 434–442.
[27] G. Tremiliosi-Filho, L.H. Dall'Antonia, G. Jerkiewicz, J. Electroanal. Chem. 422 (1997) 149–159.
[28] P.I. Iotov, S.V. Kalcheva, J. Electroanal. Chem. 442 (1998) 19–26.

[29] C. Comninellis, C. Pulgarin, J. Appl. Electrochem. 21 (1991) 703–708.
[30] F. Beck, Electrochim. Acta 33 (1988) 839–850.
[31] K.W. Willman, R.W. Murray, Anal. Chem. 55 (1983) 1139–1142.
[32] B.K. Jena, C.R. Raj, Anal. Chem. 78 (2006) 6332–6339.
[33] L. Tang, G.M. Zeng, G.L. Shen, Y. Zhang, Y.P. Li, C.Z. Fan, C. Liu, C.G. Niu, Anal. Bioanal. Chem. 393 (2009) 1677–1684.
[34] J. Tian, S.Y. Deng, D.L. Li, S. Shan, W. He, X.J. Zhang, Y. Shi, Biosens. Bioelectron. 49 (2013) 466–471.
[35] C.S. Shan, H.F. Yang, D.X. Han, Q.X. Zhang, A. Ivaska, L. Niu, Biosens. Bioelectron. 25 (2010) 1504–1508.
[36] Z. Li, Y. Huang, L. Chen, X.L. Qin, Z. Huang, Y.P. Zhou, Y. Meng, J. Li, S.Y. Huang, Y. Liu, W. Wang, Q.J. Xie, S.Z. Yao, Sens. Actuators B: Chem. 181 (2013) 280–287.
[37] A. Jiménez, M.P.G. Armada, J. Losada, C. Villena, B. Alonso, C.M. Casado, Sens. Actuators B: Chem. 190 (2014) 111–119.
[38] E.H. Hua, L. Wang, X.Y. Jing, C.T. Chen, G.M. Xie, Talanta 111 (2013) 163–169.
[39] G.M. Wen, Z.P. Li, M.M.F. Choi, J. Food Eng. 118 (2013) 56–61.